J Solid State Electrochem (2010) 14:1213–1219
DOI 10.1007/s10008-009-0966-3

ORIGINAL PAPER

Electrocatalytic activity and stability of Ti/IrO_2+MnO_2 anode in 0.5 M NaCl solution

Xian-Liang Zhou · Zhi-Guo Ye · Xiao-Zhen Hua · Ai-Hua Zou · Ying-Hu Dong

Received: 4 August 2009 / Revised: 9 October 2009 / Accepted: 20 October 2009 / Published online: 5 November 2009

Abstract Ti/IrO_2(x)+MnO_2(1-x) anodes have been fabricated by thermal decomposition of a mixed H_2IrCl_6 and Mn$(NO_3)_2$ hydrosolvent. Cyclic voltammetry (CV) and polarization curve have been utilized to investigate the electrochemical behavior and electrocatalytic activity of Ti/IrO_2(x)+MnO_2(1-x) anodes in 0.5 M NaCl solution (pH=2). Ti/IrO_2+MnO_2 anode with 70 mol% IrO_2 content has the maximum value of q^*, indicating that Ti/IrO_2(0.7)+MnO_2(0.3) anode has the most excellent electrocatalytic activity for the synchronal evolution of Cl_2 and O_2 in dilute NaCl solution. Tafel lines displayed two distinct linear regions with one of the slope close to 62 mV dec^{-1} in the low potential region and the other close to 295 mV dec^{-1} in the high potential region. Electrochemical impedance spectroscopic is employed to investigate the impedance behavior of Ti/IrO_2(x)+MnO_2(1-x) anodes in 0.5 M NaCl solution. It is observed that as the R_{ct}, R_s and R_f values for Ti/IrO_2(0.7)+MnO_2(0.3) anode become smaller, electrocatalytic activity of Ti/IrO_2(0.7)+MnO_2(0.3) anode becomes better than that of other Ti/IrO_2+MnO_2 anodes with different compositions. Ti/IrO_2(0.7)+MnO_2(0.3) anode fabricated at 400 °C has been observed to possess the highest service life of 225 h, whereas the accelerated life test is carried out under the anodic current of 2 A cm^{-2} at the temperature of 50 °C in 0.5 M NaCl solution (pH=2).

X.-L. Zhou
Key Laboratory of Nondestructive Test, Ministry of Education,
Nanchang 330063, People's Republic of China

X.-L. Zhou · Z.-G. Ye (✉) · X.-Z. Hua · A.-H. Zou · Y.-H. Dong
School of Material Science and Engineering,
Nanchang HanKong University,
696#, FengHeNan Road,
Nanchang 330063, People's Republic of China
e-mail: yezhiguo2008@163.com

Keywords Anode materials · IrO_2+MnO_2 anode, electrocatalytic activity · Stability · Dilute chloride electrolyte

Introduction

Dimensionally stable anodes (DSA) have been used extensively in dilute chloride electrolyte for disinfecting purposes and wastewater treatment [1–5]. It has already been demonstrated that the addition of chloride ions in an electrolyte results in an increase in the removal efficiency, and the complete degradation of pollutants owing to the participation of active chlorine in the form of chlorine, HClO and ClO^- [2–4, 6]. Although DSA have excellent characteristics in dilute chloride electrolyte for disinfecting and wastewater treatment, however, in order to render them more appropriate for industrial use, they must have excellent electroactivity and stability. The long-term stability of anodes for electrolysis and electrosynthesis is the most fundamental and important property that must be satisfied for any industrial application [7–11]. Poor electrocatalytic activity culminates in much more consumption of electric energy during the process of electrolysis [12–14]. Unlike the RuO_2+TiO_2 and IrO_2+Ta_2O_5 anodes, which have been utilized independently for Cl_2 and O_2 evolution, the anodes used in dilute chloride electrolyte undergo a more severe environment due to the synchronal evolution of Cl_2 and O_2 gases [1–6]. Highly stable anode materials such as PbO_2 and particularly boron doped diamond (BDD) electrodes can yield complete decolorization and mineralization of dyeing solutions owing to the efficient mediated oxidation specially with heterogeneous OH^- formed at water discharge potentials [15, 16]. However, PbO_2 anode cannot be a replacement on account of its capability to cause environmental pollution. While, on the other hand, electrocatalytic activity and

stability of BDD electrodes are not so appropriate to render them useful for industrial application such as organic degradation.

Conventional RuO_2+TiO_2 and IrO_2+Ta_2O_5 anodes have excellent electrocatalytic activity and stability for Cl_2 and O_2 evolution independently, but their service life in dilute chloride electrolyte is very short due to harsh environment exposure [17]. Therefore, it is indispensable to develop a new material or approach to improve the electrocatalytic activity and the stability of anodes in dilute chloride solution. In our previous study, it is concluded that Ti/IrO_2+MnO_2 anode used for oxygen evolution reaction (OER) demonstrates an excellent electrocatalytic performance and possesses high stability for O_2 evolution in 0.5 M H_2SO_4 solution [11, 18, 19].

In this work, considering all discussed above, Ti/$IrO_2(x)$+$MnO_2(1\text{-}x)$ anodes are fabricated by thermal decomposition of a hydrosolvent which is composed of the mixture of H_2IrCl_6 and $Mn(NO_3)_2$ at 400 °C. The influence of coating compositions on the electrochemical performance and stability of Ti/$IrO_2(x)$+$MnO_2(1\text{-}x)$ anodes in 0.5 M NaCl solution (pH=2) have been investigated by cyclic voltammetry (CV), polarization curve, electrochemical impedance spectroscopic (EIS), and accelerated service life test.

Experimental

Electrode preparation

Electrodes of nominal composition $IrO_2(x)$+$MnO_2(1\text{-}x)$, where $\leq 0 x \leq 1$, changed to 10 mol% ($\leq$10 mol% $x \leq$100 mol%) steps, were prepared by thermal decomposition of a mixture of H_2IrCl_6 (J&K Chemical Ltd.) and $Mn(NO_3)_2$ (J&K Chemical Ltd.) dissolved in hydrosolvent with different mole ratios [11]. Nine different Mn^{2+}/Ir^{4+} mole ratios (a) 1:9, (b) 2:8, (c) 3:7, (d) 4:6, (e) 5:5, (f) 6:4, (g) 7:3, (h) 8:2, and (j) 9:1, were used. For the sake of comparison, the hydrosolvent containing only single Ir^{4+} ions was also prepared. The total metal concentration of the precursor was kept around 0.2 M. The titanium plates of dimension 17×15×1.5 mm were subjected to surface pretreatment by sandblasting, degreasing with isopropanol and subsequently etching in boiling 10% oxalic acid for 30 min to get uniform roughness of surface. The precursor solution was painted by brush on both sides of the titanium plates and subsequently, the coating was dried at 100 °C for 10 min and then fired at a proper temperature for 10 min. The whole procedure was repeated until the desired loading of oxides was obtained (9 g m^{-2}, depending on composition). The final calcination was extended to 1 h for complete oxidation of the coating at 400 °C. All samples were calcined in air.

Electrode performance testing

All electrochemical studies were carried out by using aqueous 0.5 M NaCl solution (pH=2) at 25 °C, and operation was performed in a three-compartment glass cell. A platinum plate (>2 cm^2) was used as the counter electrode, and KC1 saturated calomel electrode (SCE) as the reference. PAR instrument was used throughout the experiment. The solutions were preelectrolyzed by double platinum electrodes at 1 mA cm^{-2} for 10 h before each measurement and stirring was carried out by bubbling nitrogen during the experiment. The EIS measurements were conducted on the EG&G model 273A potentiostat/galvanostat in combination with a PAR model 5310 lock-in ampliher having the frequency range of 10 mHz~100 kHz in the potential of 0.8 V(vs. SCE). A 5 mV amplitude of sinusoidal potential perturbation was employed. Cyclic voltammetry curves were used to characterize the electrochemical behavior of oxide electrodes at 20 mV s^{-1} potential with sweep rates covering a potential range between 0 and 1 V (vs. SCE). Anodic polarization curves were measured under a sweep rate of 0.5 mV s^{-1}. The specimens were held in a specially designed specimen holder and were exposed to the testing environment with the exposure surface area of ca. 1.0 cm^2. In order to avoid significant temperature rise during the accelerated electrolysis tests, a large testing cell with a working volume of 1,000 cm^3 was used.

The accelerated lifetime was measured in the 0.5 M NaCl solution (pH=2) at 50 °C with a constant anodic current density of 2 A cm^{-2}. During the testing process of the accelerated lifetime, pH value in 0.5 M NaCl solution increased gradually and Cl^- concentration decreased gradually. In order to keep the stability of pH value and Cl^- concentration, the accelerated lifetime for Ti/IrO_2+MnO_2 anode was measured in 0.5 M NaCl solution with a big working volume of 20 L, and pH value was adjusted by 0.5 M H_2SO_4 solution and 0.5 M NaOH solution at an interval of 0.5 h. The testing solution was replaced every 10 h. When bath voltage between working and counter electrode increases up to 5 V, comparing from the initial voltage, this test was assumed to be complete.

Results and discussion

Voltammetric characteristics

Cyclic voltammetry can be considered to be an ideal "in situ" measuring technique, since it can investigate the surface behavior of an electrode sensitively by cyclic voltammograms. Figure 1 depicts the typical CV curves for Ti/$IrO_2(x)$+$MnO_2(1\text{-}x)$ anodes. These curves show a

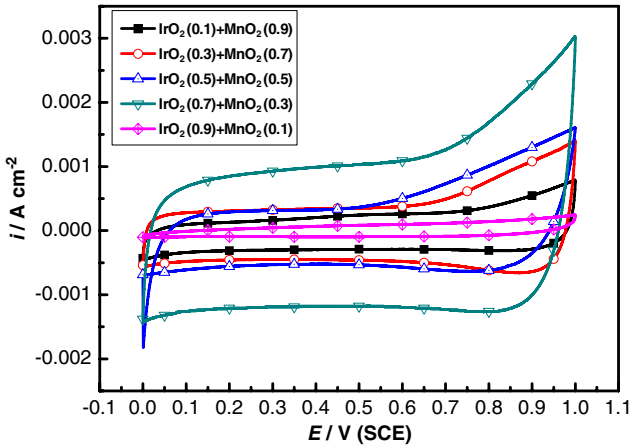

Fig. 1 Cyclic voltammograms for Ti/IrO_2(x)+MnO_2(1-x) anodes in 0.5 M NaCl solution at 20 mV s^{-1}

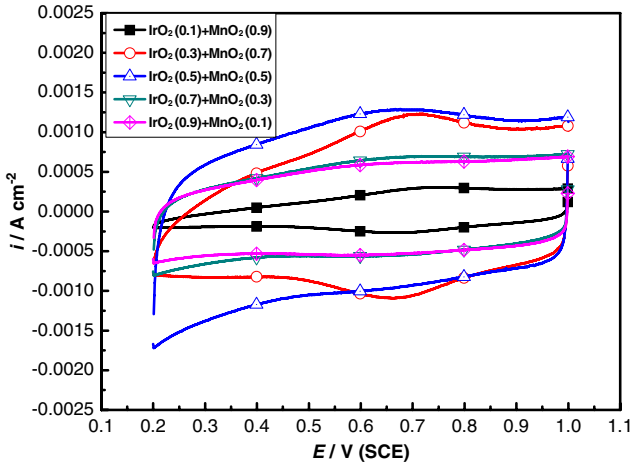

Fig. 2 Cyclic voltammograms for Ti/IrO_2(x)+MnO_2(1-x) anodes in 0.5 M H_2SO_4 solution at 20 mv s^{-1}

potential range of 0–1.0 V (SCE) as a function of composition in 0.5 M NaCl solution. As shown in Fig. 1, it is quite obvious that the voltammetric current of Ti/IrO_2+MnO_2 anode with 70 mol% IrO_2 content is greater than that of other anodes. The anodes with different IrO_2 contents exhibit a voltammogram typical of the DSA-type oxide electrodes with a pseudocapacitive behavior. While, the electrochemical response is typical of a capacitor exhibiting accurately rectangular mirror images and rapid reversals of directions of response currents. The redox process of the Ti/IrO_2(x)+MnO_2(1-x) anodes is attributed to the Ir^{III}/Ir^{IV} solid state redox transitions and the proton injection (or ejection), thus compensating for the change of the charge of the oxide film. In Fig. 1, it is quite evident that the voltammetric curves of Ti/IrO_2(x)+MnO_2(1-x) anodes between 0 and 1 V (vs. SCE) does not contain any visible redox couple of current peaks. When scan potential reaches beyond 0.6 V (vs. SCE), a sharp increase in the anodic current density of Ti/IrO_2+MnO_2 anodes has been observed with an increase in scan potential between 0.6 and 1.0 V (vs. SCE). Invisibility of a couple of current peaks in all CV curves may be ascribed to the increase of anodic current density due to the low evolution potential for Cl_2 gas. This phenomenon is quite contrary to the behavior exhibited by the voltammetric curves of Ti/IrO_2(x)+MnO_2(1-x) anodes in 0.5 M H_2SO_4 solution. It is manifested in Fig. 2 that Ti/IrO_2(x)+MnO_2(1-x) anodes in 0.5 M H_2SO_4 solution possess a couple of current peaks in all CV curves between 0.6 and 0.8 V (vs. SCE). Especially, it is clearly visible on the CV curve of Ti/IrO_2(0.3)+MnO_2(0.7) anode, which has also been illustrated in our previous work [11]. Both IrO_2 and RuO_2-type electrodes have been shown to emerge the same redox peak during the process of oxygen reduction, which may be due to the conversion of the active components such as $Ir^{III}\rightleftarrows Ir^{IV}$ and $Ru^{III}\rightleftarrows Ru^{IV}$ [20–23]. Therefore, Ti/IrO_2+MnO_2 anodes in 0.5 M H_2SO_4 solution are only subjected to the oxygen evolution reaction, but in 0.5 M NaCl solution, it undergoes the synchronal evolution of both Cl_2 and O_2 gases.

The number of electrochemical active sites can be described generally by the voltammetric charge, i.e., q^*, which is measured by graphical integral of cyclic voltammogram in the electric double layer of O_2 and Cl_2 evolution [9, 24]. Figure 3 shows the dependence of q^* values covering the potential region between 0 and 1 V (vs. SCE) on the composition of Ti/IrO_2(x)+MnO_2(1-x) anodes at 20 mV s^{-1} potential sweep rate in 0.5 M NaCl solution. It is obvious that the q^* value increases gradually with an increase in IrO_2 contents up to 50 mol%. When IrO_2 contents reach beyond 50 mol%, the q^* value increases rapidly and reaches the maximum (IrO_2 content=70 mol%). With a further increase in IrO_2 contents, the q^* value descend abruptly. Therefore, it is concluded that Ti/IrO_2+

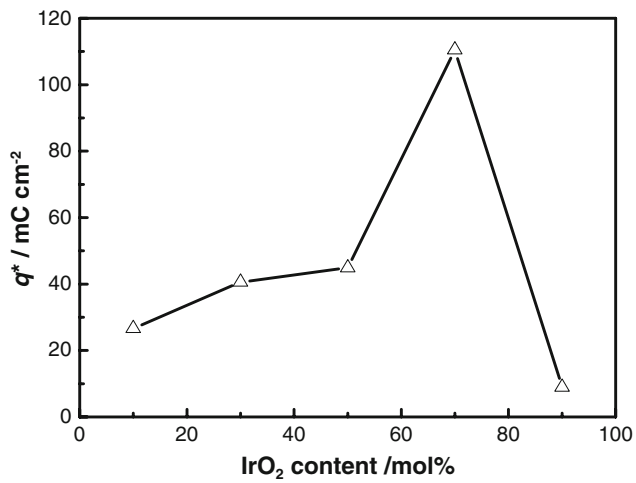

Fig. 3 Dependence of voltammetric charge q^* on the composition of Ti/IrO_2(x)+MnO_2(1-x) anodes in 0.5 M NaCl solution at 20 mv s^{-1}

MnO_2 anode with 70 mol% IrO_2 content has the maximum value of q^*, indicating that Ti/IrO_2(0.7)+MnO_2(0.3) anode has the most excellent electrocatalytic activity for the synchronal evolution of Cl_2 and O_2 in dilute NaCl solution. Variation of the q^* value may be related to the effective surface area of Ti/IrO_2+MnO_2 anodes with different compositions. Figure 4 illustrates the surface micrographs of Ti/IrO_2+MnO_2 anodes with 30 and 70 mol% IrO_2 contents fabricated at 400 °C. The white nanoprecipitates consist of pure IrO_2 phase [11]. Since the anode surface with 30 mol% IrO_2 contents contains few IrO_2 precipitates, therefore, its effective surface area is lower than that of the other anodes. Consequently, the response sites at the anode with 30 mol% IrO_2 content become less in terms of the q^* value. When the IrO_2 contents become equal to 70 mol% in the coating, the mass of nano-IrO_2 poles separates out on the coating surfaces that can significantly promote the augmentation in the effective surface area of the anodes. In our previous work [11], Ti/IrO_2+MnO_2 anode with 50 mol% IrO_2 contents in 0.5 M H_2SO_4 solution has the maximum value of q^*, while in our present work, Ti/IrO_2+MnO_2 anode with 70 mol% IrO_2 content in 0.5 M NaCl solution has the maximum value of q^*. This behavior may be attributed to the simultaneous Cl_2 and O_2 evolution and Cl^- adsorption at the anode surface in 0.5 M NaCl solution. In addition, Ti/IrO_2(x)+MnO_2(1-x) anodes in 0.5 M H_2SO_4 solution only involve the O_2 evolution reaction [11].

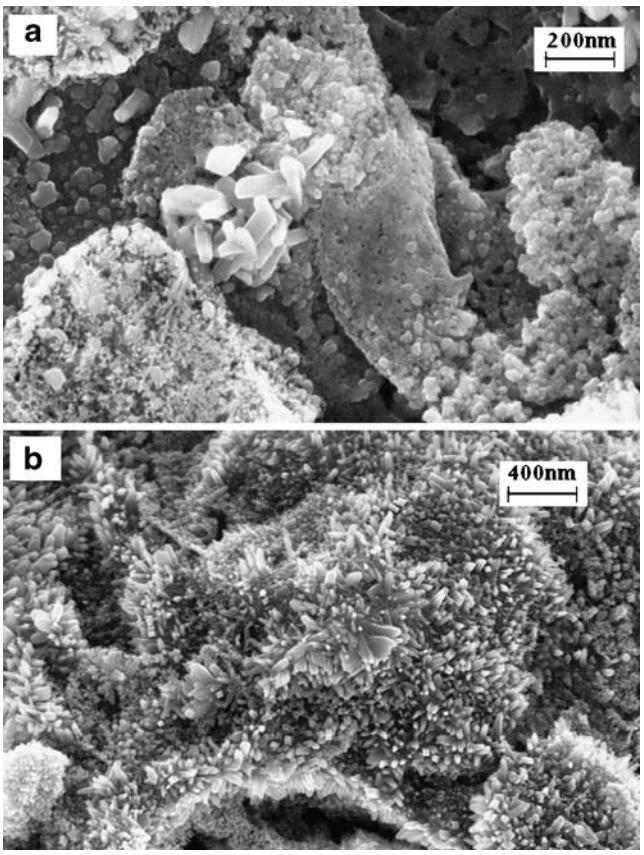

Fig. 4 Surface micrographs of Ti/IrO_2(x)+MnO_2(1-x) coatings with different compositions prepared at 400 °C, **a** Ti/IrO_2(0.3)+MnO_2(0.7), **b** Ti/IrO_2(0.7)+MnO_2(0.3)

Polarization curves

Unlike the RuO_2+TiO_2 and IrO_2+Ta_2O_5 anodes for Cl_2 and O_2 evolution independently, the anodes used in dilute chloride electrolyte undergo the synchronal evolution of Cl_2 and O_2 gases. Figure 5 displays the iR_s-corrected anodic polarization curves of Ti/IrO_2(x)+MnO_2(1-x) anodes in 0.5 M NaCl solution. During the process of O_2 and Cl_2 synchronal evolution, composition of IrO_2+MnO_2 coating does not have any significant effect on Tafel slopes b of Ti/IrO_2+MnO_2 anodes in low and high potential regions, as shown in Fig. 5. Composition influence of IrO_2+MnO_2 coating on the Tafel slopes b in dilute NaCl solution is the same as that of IrO_2+MnO_2 coating in 0.5 M H_2SO_4 solution [11]. It is evident that Ti/IrO_2+MnO_2 anodes with various IrO_2 contents present the phenomena of double Tafel slopes at the low and high potential regions of polarization curves. Double Tafel slopes of anode materials are generally characterized by the change of the rate determining step during the gas evolution reaction [9, 11]. Ti/RuO_2-based composite anodes have been observed to exhibit the same behavior of double Tafel slopes during the process of Cl_2 evolution [25].

The reaction mechanism of O_2 evolution at Ti/IrO_2+MnO_2 anodes in 0.5 M H_2SO_4 solution has been investigated in our previous study [11]. In the low potential region, the OER for 0.5 M H_2SO_4 is completely controlled by step ($S-OH_{ads}^* \rightarrow S-OH_{ads}$) and theoretical Tafel slope is measured to be 60 mV. In the high potential region, step ($S+H_2O \rightarrow S-OH_{ads}^*+H^++e^-$) becomes the rate deter-

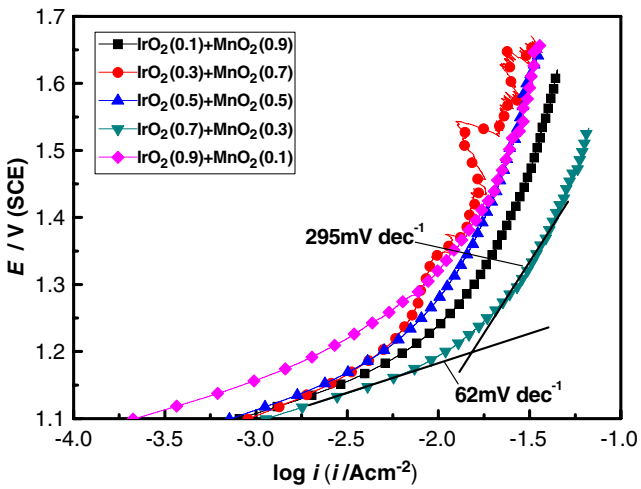

Fig. 5 Anodic polarization curves for Ti/IrO_2(x)+MnO_2(1-x) anodes in 0.5 M NaCl solution

mining step of the OER and theoretical Tafel slope is calculated to be 125 mV dec^{-1}. Chlorine evolution of metal oxide anode in saturated NaCl solution generally takes place according to the reactions ($S+Cl^- \rightarrow SCl+e^-$ and $SCl+Cl^- \rightarrow Cl_2+2S+e^-$) or ($S+Cl^- \rightarrow SCl+e^-$ and $2SCl \rightarrow Cl_2+2S$) [26, 27]. When the second electron transfer becomes rate-limiting, the Tafel slope comes out to be about 40 mV and about 30 mV for the reactions, respectively. As shown in Fig. 5, the Tafel line has a slope of 62 mV dec^{-1} in the low potential region, which is in complete accordance with the theoretical Tafel slope of step ($S-OH_{ads}^* \rightarrow S-OH_{ads}$) for O_2 evolution reaction. Hence, for the low potential region, step ($S-OH_{ads}^* \rightarrow S-OH_{ads}$) becomes the rate determining step of Ti/IrO_2+MnO_2 anodes for synchronal evolution reaction of Cl_2 and O_2 gases in 0.5 M NaCl solution. In the high potential region, the Tafel line displays a slope of 295 mV dec^{-1}, which is comparatively much greater than the theoretical Tafel slopes of all the steps. This phenomenon indicates that the present reaction mechanism is not appropriate to illustrate the synchronal evolution reaction of Cl_2 and O_2 gases in dilute NaCl solution in the high potential region.

In addition, polarization curve of Ti/IrO_2+MnO_2 anode with 30 mol% IrO_2 content displays an irregular behavior in the high potential region, indicating the instability of Ti/IrO_2(0.3)+MnO_2(0.7) anodes in 0.5 M NaCl solution. In Fig. 4a, it is clear that IrO_2+MnO_2 coating with 30 mol% IrO_2 content is loose and uneven, that can result in a big fluctuation in the current density owing to the coating dissolution and abscission during the process of Cl_2 and O_2 evolution caused by the severe impact of O_2 bubbles.

EIS analysis

Figure 6 demonstrates the experimental and fitted EIS patterns for Ti/IrO_2+MnO_2 with 70 mol% IrO_2 content in 0.5 M NaCl solution at 0.8 V (vs. SCE). The shapes of EIS curves for anodes with various IrO_2 contents (10, 30, 50, 70, and 90 mol%) have close resemblance to one another, therefore, here, only the pattern for Ti/IrO_2(0.7)+MnO_2(0.3) anode is discussed. In Fig. 6a, the complex planes in the whole frequency domain show two capacitance arcs. The arc in the low-frequency domain of the complex plane is characterized by a semicircle being attributed to the electrochemical reaction at the interface between oxide layer and solution. The other arc in the intermediate and high-frequency domain only shows a part of the semicircle that is related to the physical response of porous structure of oxide electrodes observed. Figure 6b depicts the presence of two phase angle peaks lying in the low- and high-frequency domains. Two phase angle peaks indicate that the Ti/IrO_2+MnO_2 anodes in 0.5 M NaCl have two time constants and two capacitance arcs.

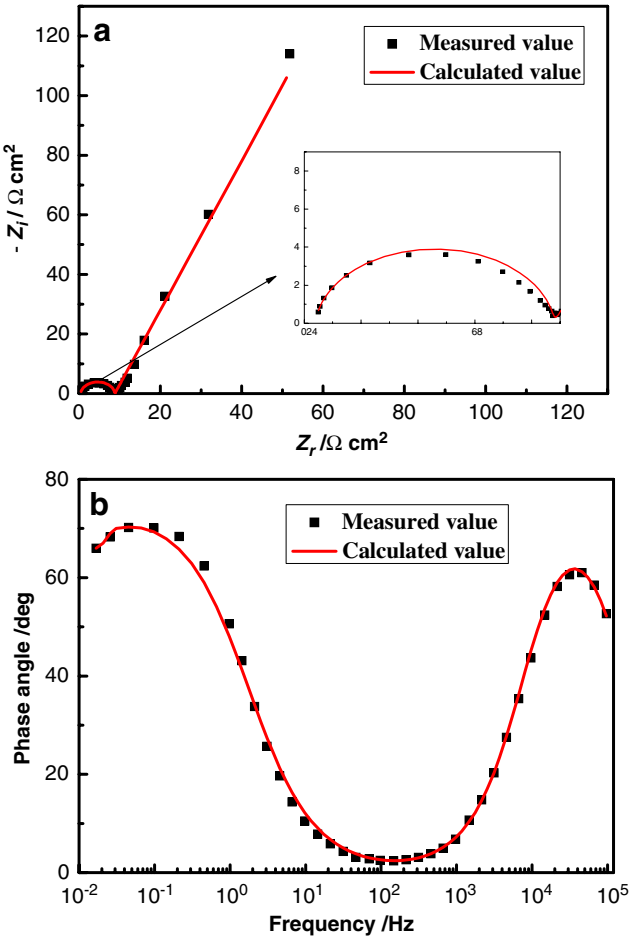

Fig. 6 Experimental and fitted EIS patterns for Ti/IrO_2+MnO_2 with 70 mol% IrO_2 contents in 0.5 M NaCl solution at 0.8 V (vs. SCE): **a** Nyquist diagrams; and **b** Bode plots

The equivalent circuit, EEC, can be characterized as $R_s(R_fQ_f)(R_{ct}Q_{dl})$ (see Fig. 7). In the previous literature, it is quite often to simulate the impedance data for metal oxide anodes [28–30]. The (R_fQ_f) and ($R_{ct}Q_{dl}$) combinations have been observed in high- and low-frequency domains of the impedance spectroscopy. R_f is the resistance and Q_f is the capacitance of oxide layer. The (R_fQ_f) combination symbolizes the physical response of porous structure of oxide electrodes observed in the intermediate and high frequency domain and independent of the reaction potential. The ($R_{ct}Q_{dl}$) combination definitely relates to

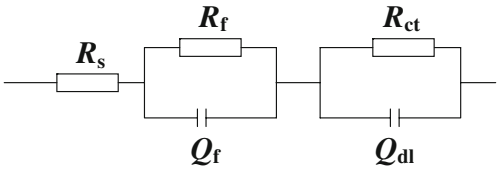

Fig. 7 The equivalent circuit for Ti/IrO_2(x)+MnO_2(1-x) anodes with various compositions in 0.5 M NaCl solution at 0.8 V (SCE)

the electrochemical reaction of Cl_2 and O_2 synchronal evolution in the low-frequency loop. R_{ct} is the response resistance for Cl_2 and O_2 evolution reaction and Q_{dl} is the surface capacitance. R_s stands for the uncompensated resistance that includes both the solution resistance and the resistance of interfacial insulate TiO_2 film formed by the oxidation of Ti substrate [11, 31].

Figure 6 also gives the calculated impedance spectra by using the EEC of $R_s(R_fQ_f)(R_{ct}Q_{dl})$. An excellent adjustment ($x^2<10^{-3}$) has been achieved. As shown in Fig. 6, the simulated Nyqusit and Bode plots are in complete harmony to the measured ones, suggesting that the EEC is basically compatible with the coating nature during the process of gases evolution. The fitted electrical parameters are listed in Table 1.

As shown in Table 1, the R_s and R_f values descend gradually with an increase in IrO_2 contents. When IrO_2 contents become equal to 70 mol%, the R_s and R_f values synchronously reach the minimum. On the contrary, the R_s and R_f values increase with a further increase in IrO_2 contents. The minimal R_s values indicate that Ti/IrO_2(0.7)+MnO_2(0.3) anode has the minimal uncompensated resistance that includes both the solution resistance and the resistance of interfacial insulate TiO_2 film formed by the oxidation of Ti substrate. The minimal R_f values demonstrate that Ti/IrO_2(0.7)+MnO_2(0.3) anode possesses the minimal resistance of oxide layer. Therefore, the minimal R_s and R_f values play a beneficial role to increase the electrocatalytic activity of Ti/IrO_2(0.7)+MnO_2(0.3) anode. Table 1 shows the variation of Q_f and Q_{dl} values of Ti/IrO_2(x)+MnO_2(1-x) anodes as a function of IrO_2 contents. It is quite evident in Table 1 that the Q_f and Q_{dl} values increase gradually with an increase in IrO_2 contents. When IrO_2 contents become equal to 70 mol%, the Q_f and Q_{dl} values synchronously reach the maximum. On the contrary, the Q_f and Q_{dl} values decrease with a further increase in IrO_2 contents. In one of our previous work [19], the $1/R_{ct}$ and Q_{dl} can reliably evaluate and explain the electrocatalytic activity of oxide electrodes. Hou et al. [30] have also demonstrated the fact that the magnitude of parameters Q_{dl} can reliably evaluate the electrocatalytic activity of oxide electrodes. Therefore, the maximal Q_f and Q_{dl} values indicate that Ti/IrO_2+MnO_2 anode with 70 mol% IrO_2 contents has the most excellent electrocatalytic activity than that of other Ti/IrO_2+MnO_2 anodes with different IrO_2 contents. Table 1 shows the variation of R_{ct} values of Ti/IrO_2(x)+MnO_2(1-x) anodes as a function of IrO_2 contents. R_{ct} is termed as the response resistance for Cl_2 and O_2 evolution reaction. More enhanced electrocatalytic activity for Ti/IrO_2(x)+MnO_2(1-x) anodes in 0.5 M NaCl can be achieved by lowering the value of $R_{ct.}$ That is why, Ti/IrO_2+MnO_2 anode with 70 mol% IrO_2 contents has the smallest R_{ct} value, further justifying the fact that Ti/IrO_2(0.7)+MnO_2(0.3) has the most excellent electrocatalytic activity than that of other Ti/IrO_2+MnO_2 anode with IrO_2 contents. Previous studies [31, 32] have also testified the same phenomenon occurred at Ti/IrO_2+Ta_2O_5 anodes.

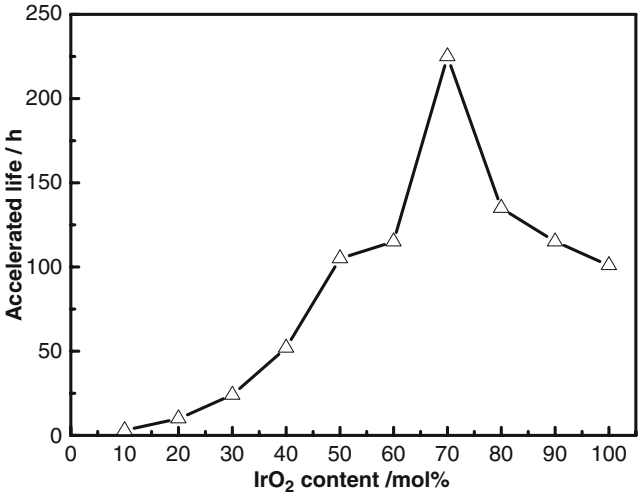

Fig. 8 Accelerated life of Ti/IrO_2(x)+MnO_2(1-x) anodes in 0.5 M NaCl solution

Accelerated service life

The accelerated life test is performed under the anodic current of 2 A cm^{-2} at the temperature of 50 °C in 0.5 M NaCl solution. This test has been used to predict the long-term stability of the Ti/IrO_2(x)+MnO_2(1-x) anodes prepared at 400 °C. When bath voltage between working and counter electrode is increased up to 5 V as compared with the initial bath voltage, this test is assumed to be complete. The

Table 1 Summary of fitted EIS data for Ti/IrO_2(x)+MnO_2(1-x) anodes with different IrO_2 contents recorded at 0.8 V(vs. SCE)

IrO_2 content, mol%	R_S, Ω cm^2	R_f, Ω cm^2	$10^5\times(Q_f)$, Ω^{-1} cm^{-2} s^n	n_f	$10^{-5}\times R_{ct}$, Ω cm^2	Q_{dl}, Ω^{-1} $cm^{-2}s^n$	n_{dl}
10	0.7314	12.98	2.046	0.97	59.1	0.00986	0.84
30	0.5855	12.34	2.367	0.97	11.0	0.01979	0.81
50	0.6089	9.807	2.566	0.97	11.6	0.02744	0.78
70	0.3946	8.381	4.463	0.95	3.96	0.04068	0.76
90	0.4343	10.35	3.99	0.95	4.81	0.002625	0.70

obtained lifetime data is represented as a function of IrO_2 contents in Fig. 8. When the IrO_2 contents of the coating is less than 30 mol%, the service life of Ti/IrO_2(x)+MnO_2(1-x) anodes has been observed to be short and slowly increases with the increase in IrO_2 contents of the coating as clearly shown in the figure. The short service life may be the consequence of the high resistivity [11] of the IrO_2(0.1)+MnO_2(0.9) and IrO_2(0.3)+MnO_2(0.7) coatings, since high resistivity can easily lead to an insulating rutile TiO_2 film generated at the interface of Ti-substrate and oxide coating. When IrO_2 contents of the coating become higher than 30 mol%, the service life rapidly increases with an increase in IrO_2 contents. It is found that the highest service life of 225 h is achieved with the IrO_2 contents of 70 mol% and descends after the IrO_2 contents reach beyond 70 mol%. In our previous work [11], it has been discovered that the preferential orientation of IrO_2 (101) plane is quite favorable to the stability of Ti/IrO_2(x)+MnO_2(1-x) electrodes. IrO_2 (101) plane of Ti/IrO_2(0.7)+MnO_2(0.3) anode has been observed to be the plane of the highest preferential orientation [11], which is interrelated with its highest service life for Ti/IrO_2+MnO_2 anode in 0.5 M NaCl pH 2 solution.

Conclusion

An investigation about the electrocatalytic activity and stability of Ti/IrO_2(x)+MnO_2(1-x) anodes prepared at 400 °C in 0.5 M NaCl solution has been carried out in this work. The q^* value increases gradually with an increase in IrO_2 contents. It is concluded that when the IrO_2 contents reach beyond 50 mol%, the q^* value increases rapidly and reaches the maximum (IrO_2 content=70 mol%). While, a further increase in IrO_2 contents result in a sharp decrease in the q^* value. Ti/IrO_2(0.7)+MnO_2(0.3) anode has been found to possess the most excellent electrocatalytic activity for the synchronal evolution of Cl_2 and O_2 in dilute NaCl solution. Mass of nano-IrO_2 poles separates out at the coating surfaces of Ti/IrO_2(0.7)+MnO_2(0.3) anode that can significantly promote the effective surface area of the anodes. Tafel lines display two distinct linear regions with one of the region has the slope of about 62 mV dec^{-1} in the low potential region and the other has about 295 mV dec^{-1} in the high potential region. Ti/IrO_2(0.7)+MnO_2(0.3) anode has the maximum values of Q_f and Q_{dl}, indicating that Ti/IrO_2(0.7)+MnO_2(0.3) has the most excellent electrocatalytic activity than that of other Ti/IrO_2+MnO_2 anodes with different compositions. The highest service life of 225 h has been recorded for Ti/IrO_2(0.7)+MnO_2(0.3) anode prepared at 400 °C has IrO_2(101) plane of Ti/IrO_2(0.7)+MnO_2(0.3) anode and has the highest preferential orientation that is quite favorable and beneficial to the stability of Ti/IrO_2(x)+MnO_2(1-x) electrodes.

Acknowledgements This project is financially supported by National Natural Science Foundation of China (50871051), Natural Science Foundation of JiangXi Province Education Department (CB200600003), and Key Laboratory of Nondestructive Test, Ministry of Education (ZD200729003). Grateful acknowledgement goes to them!

References

1. Wang XM, Hu JM, Zhang JQ, Cao CN (2008) Electrochim Acta 53:3386
2. Shi HX, Qu JH, Wang AM, Ge JT (2005) Chemosphere 60:326
3. Trasatti S (2000) Electrochim Acta 45:2377
4. Hernlem BJ (2005) Water Res 39:2245
5. Panizza M, Cerisola G (2004) Electrochim Acta 49:3221
6. Hu CZ, Liu HJ, Qu JH (2005) Colloid Surface A 260:109
7. Beck F (1989) Electrochim Acta 34:811
8. Beck F (1989) Corros Sci 29:379
9. Trasatti S (1980) Electrodes of conductive metallic oxides. Elsevier, Amsterdam
10. Hu JM, Meng HM, Zhang JQ, Cao CN (2002) Corros Sci 44:1655
11. Ye ZG, Meng HM, Chen D, Yu HY, Huan ZS, Wang XD, Sun DB (2008) Solid State Sci 10:346
12. Zhang ZX (2005) Engineering of titanium electrode. Metallurgical Industry Press, Beijing
13. Wu BL, Lincot D, Vedel J, Yu LT (1997) J Electroanal Chem 420:159
14. Fujimura K, Matsui T, Izumiya K, Kumagai N, Akiyama E, Habazaki H, Kawashima A, Asami K, Hashimoto K (1999) Mater Sci Eng A 267:254
15. Andrade LS, Tasso TT, Da Silva DL, Rocha-Filho RC, Bocchi N, Biaggio SR (2009) Electrochim Acta 54:2024
16. Ramesham R (1998) Thin Solid Films 322:158
17. Da Silvaa LM, Fernandesb KC, De Fariab LA, Boodts JFC (2004) Electrochim Acta 49:4893
18. Ye ZG, Meng HM, Sun DB (2008) Electrochim Acta 53:5639
19. Ye ZG, Meng HM, Sun DB (2008) J Electroanal Chem 621:49
20. Burke LD, Whelan DP (1984) J Electroanal Chem 162:121
21. Pickup PG, Birss VI (1988) J Electroanal Chem 240:185
22. Angelinetta C, Trasatti S, Atanasoska L, Atanasoski R, Miesvski Z (1989) Mater Chem Phys 22:231
23. Atanasoska L, Atanasoski R, Trasatti S (1990) Vacuum 40:91
24. Durke LD, Murphy OJ (1979) J Electroanal Chem 96:19
25. Hu JM, Zhang JQ, Cao CN (2004) Int J Hydrogen Energy 29:791
26. Santana MHP, De Faria LA (2006) Electrochim Acta 51:3578
27. Cornell A, Håkansson B, Lindbergh G (2003) Electrochim Acta 48:473
28. Jin SX, Ye SY (1996) Electrochim Acta 41:827
29. Alves VA, Da Silva LA, Boodts JFC (1998) Electrochim Acta 44:1525
30. Hou YY, Hu JM, Liu L, Zhang JQ, Cao CN (2006) Electrochim Acta 51:6258
31. Hu JM, Zhang JQ, Meng HM, Zhang JQ, Cao CN (2005) Electrochim Acta 50:5370
32. Rajkumar D, Song BJ, Kim JG (2007) Dyes Pigm 7:21